

## Spectroelectrochemical Dynamics of Dendritic Poly (Propylene imine)-Polythiophene Star Copolymer Aptameric 17 $\beta$ -Estradiol Biosensor

Rasaq A. Olowu, Peter M. Ndangili, Abd Almonam Baleg, Chinwe O. Ikpo, Njagi Njomo, Priscilla Baker, Emmanuel Iwuoha\*

SensorLab, Department of Chemistry, University of the Western Cape, Bellville, 7535, South Africa

\*E-mail: [eiwuoha@uwc.ac.za](mailto:eiwuoha@uwc.ac.za)

Received: 20 February 2011 / Accepted: 4 March 2011 / Published: 1 May 2011

---

Aptamers, which are in vitro-selected functional oligonucleotides, have been employed to design novel aptasensor due to their inherent high selectivity and affinity compared to traditional biorecognition elements. This report presents a novel aptamer biosensor for determining the endocrine disrupting compound (EDC), 17 $\beta$ -estradiol (E2), which was constructed from a SELEX-synthesized 76-mer biotinylated aptamer for 17 $\beta$ -estradiol incorporated in a dendritic generation 1 poly(propylene imine)-polythiophene (G1PPT-co-PEDOT) star copolymer-functionalised Au electrode via biotin-avidin interaction. The sensor platform and aptasensor were interrogated with scanning electron microscopy (SEM), FTIR, electrochemical impedance spectroscopy (EIS), cyclic voltammetry (CV) and square wave voltammetry (SWV). The kinetic parameters of the sensor platform were determined by modelling the [Fe(CN)<sub>6</sub>]<sup>3/4-</sup> (redox probe) Nyquist and Bode impedimetric spectra to the appropriate equivalent electrical circuit. The EIS spectra shows that at low frequencies (100 mHz) when the electronics of the electrode systems are only minimally perturbed the Au|G1PPT-co-PEDOT nanoelectrode exhibited greater semi-conductor behaviour (higher phase angle value) than Au|G1PPT due to the incorporation of charged functionalized dendrimer. However, the Bode plot also shows that the charge transfer dynamics of the nanoelectrode can be frequency modulated. The biosensor response to 17 $\beta$ -estradiol was based on the decrease in the SWV current as the EDC binds to the ssDNA aptamer on the biosensor. The dynamic linear range of the sensor was 0.1 – 100 nM. These initial studies also showed that the aptamer used in this study was very selective to, and reproducible for, 17- $\beta$ -estradiol.

---

**Keywords:** Functionalized dendrimer, conducting polymer, 17 $\beta$ -estradiol (E2), star copolymer, SELEX, endocrine disrupting compound, DNA aptamer, electrochemical impedance spectroscopy,

## 1. INTRODUCTION

Aptamers are short, single stranded and artificial receptors with a special three-dimensional conformation primary RNA or DNA sequence that can bind to their targets with high affinity and selectivity [1-3]. These targets include low molecular weight organic and inorganic compound, as well as macromolecules such as drugs, proteins and even whole cells [1-2]. These properties have enabled aptamers to be widely explored as biological recognition element for specific sensing of a variety of analytes. Selectivity of the artificial receptor for the specific target is based on *in vitro* selection from random sequence nucleic acids combinatorial libraries by Systematic Evolution of Ligands by Exponential Enrichment (SELEX) [2-3]. Aptamer possess many advantages over the traditional recognition molecules such as antibodies and enzymes due to their chemical simplicity, non toxicity, specific binding ability, synthesizability, lack of immunogenicity, good stability during long-term storage and ease of modification for additional immobilization procedures [2-3]. J.E Smith and his co-workers utilized aptamer conjugated magnetic nanoparticle for the collection of cancer cell while target cell labelled with aptamer-modified fluorescence nanoparticles was required for the optical detection [4]. An aptamer based electrochemical sensor for label-free recognition and detection of cancer cell with a detection limit of  $6 \times 10^3$  cells/mL has been reported [5]. Electrochemical aptamer biosensors have started to attract attention due to the specificity of aptamer for the recognition of their target analytes.

Recently a highly sensitive, reusable aptasensor for adenosine with a detection limit of  $1.65 \times 10^{-8}$  M has been reported [6]. An aptasensor for the determination of cocaine incorporating gold nanoparticles modification have been fabricated by Xiaoxia and co workers[7]. In order to amplify signals various electrochemical aptasensor mainly based on labelled aptamers have been fabricated. The most commonly used electroactive labels are ferrocene and methylene blue. The use of labelled aptamers have been reported to affect the binding affinity of the aptamers with their target [8-9]. Consequently attentions seem to be redirected on label-free aptamer as biological recognition elements. A label-free electrochemical detection of protein based on a ferrocene-bearing cationic polythiophene and aptamer with a detection of 75 fmol has been reported [9]. Du and his co-workers developed a multifunctional label-free electrochemical biosensor for the detection of adenosine triphosphate (ATP) [10].

Dendrimers are a class of three-dimensional macromolecules with a well defined, highly branched treelike morphologies.[11-13]. The unique properties of dendrimers such as biocompatibility, controlled composition, adequate functional groups for chemical fixation, structural homogeneity makes them suitable for a wide range of biosensing applications [11-12]. Application of dendrimers in biosensor fabrication has been reported for various signal transduction modes. Zhanxia et al [11] constructed an impedimetric aptasensor based on polyamidoamine (PAMAM) dendrimer modified gold electrode for the determination of thrombin. Dendrimeric biosensors based on polyamidoamine (PAMAM) dendrimer modified with gold nanoparticle have been shown to exhibit low detection limit ( $1.4 \times 10^{-14}$  M) [14]. One of the advances in dendrimer-based sensor systems is the use of hybrid dendrimers containing encapsulated metal nanoparticles or the preparation of dendritic copolymers which make them very useful for application in catalysis and electrocatalysis [15]. The formation of

dendritic copolymers with conducting polymers such as polyaniline, polythiophene and polypyrrole should increase the conductivity and lead to nanostructuring of the product due to the elongation of the conjugation chain and an unhindered  $\pi$  stacking of the polymer molecules by the dendrimer [15-16].

This report contains the preparation of Generation 1 poly(propyleneimine)-polythiophene copolymer for application as biocompatible platform for the fabrication of aptameric biosensor for the determination of the estrogenic endocrine-disrupting compound (EDC),  $17\beta$ -estradiol which mimics endocrine activity in humans and wild life that have deleterious consequences including cancer and reproductive abnormalities [17].

Estrogens pollute municipal waste water through the discharge of human and agricultural wastes and may have serious health implications if they enter the food chain in large quantities. In South Africa, the extent of this class of pollution is not yet thoroughly studied. The aptamer biosensor provides a rapid response and easy-to-use approach for point of need assessment of EDC content of waste water, which is more cost effective than other traditional analytical methods [18-19]. Electrochemical determination of E2 has been performed on electrodes modified with poly(L-serine) [20] or with carbon nanotube and ionic liquid [21]. Since aptamers are known for their ultra-sensitivity and excellent selectivity for target analyte, biosensors containing aptamers will be one of the most reliable methods of determining estrogenic EDCs. This report deals with the construction of a Au|G1PPT-co-PEDOT star copolymer electrode system and its application in the development of aptameric biosensor by incorporating an E2-specific 76-mer biotinylated ssDNA aptamer.

## 2. EXPERIMENTAL

### 2.1. Materials and methods

Generation 1 (G1) Poly(propyleneimine) (PPI) dendrimer, 2-Thiophene carboxaldehyde, 3,4-ethylenedioxythiophene (EDOT), dichloromethane (DCM), methanol, 3,3-dithiodipropionic acid (DPA), N-(3-dimethylaminopropyl)-N-ethylcarbodiimide hydrochloride (EDAC), N-hydroxysuccinimide (NHS), streptavidin,  $17\beta$ -estradiol, sodium monohydrogen phosphate, potassium dihydrogen phosphate, lithium perchlorate, potassium ferricyanide [ $K_3Fe(CN)_6$ ] and potassium ferrioxalate [ $K_4Fe(CN)_6$ ] and sodium dodecylsulphate were bought from Sigma-Aldrich (South Africa). All chemicals were of analytical grade and were used as received.

Deionized water (18.2 M $\Omega$ ) purified by a milli-QTM system (Millipore) was used throughout the experiment for aqueous solution preparation.

A 76-mers biotinylated ssDNA aptamer synthesized by Inqaba Biotechnical Industries (Pty) Ltd., Hatfield, South Africa was used as aptamer probe. The sequence of the 76-mers sized biotinylated aptamer is given below:

5'-BiotinGCTTCCAGCTTATTGAATTACACGCAGAGGGTAGCGGCTCTGCGCATTC  
AATTGCTGCGCGCTGAAGCGCGGAAGC-3

## 2.2. Electrochemical measurement

A three electrode system was used to perform all electrochemical experiments. Gold electrode with a diameter of 1.6 mm was used as the working electrode, platinum wire as the counter electrode, and Ag/AgCl (3 M Cl) as the reference electrode. All electrochemical (voltammetric) experiments were recorded with Zahner IM6 electrochemical workstation (MeBtechnik).

Square wave voltammetry (SWV) measurement at an amplitude of 25 mV and frequency of 15 Hz, electrochemical impedance spectroscopy (EIS), and cyclic voltammetry measurements were recorded with this electrochemical workstation. All solutions were de-aerated by purging with argon through it for 20 min.

The experiments were carried out under room temperature. UV/Vis spectra measurements were recorded with the Nicolette Evolution 100 Spectrometer (Thermo Electron Corporation, UK). Fourier transform infrared (FTIR) measurements were done with PerkinElmer spectrum 100-FTIR spectrophotometer. The morphology of the samples were studied by SEM Gemini LEO 1525 model microscope. Fluorescence spectrophotometer from Horiba Nanolog<sup>TM</sup> 3-22-TRIAX with double grating excitation and emission monochromators with a slit width of 3.2 nm was employed for aqueous G1PPI, and G1PPT were used in the fluorescence experiment. <sup>1</sup>H NMR (200 MHz) (Varian GeminiXR200 spectrometer), was carried out using CDCl<sub>3</sub> as the solvent with tetramethylsilane as an internal standard.

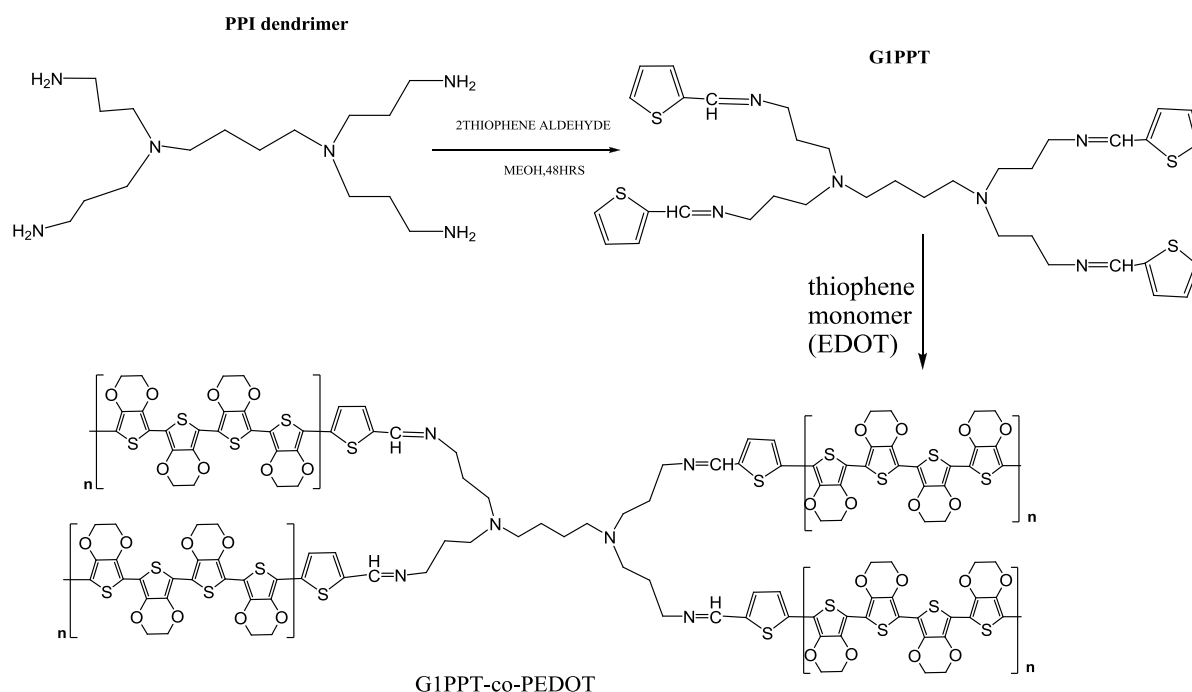
## 2.3. Synthesis of the G1 poly(propylene thiophenoimine) (G1PPT) dendrimer

Synthesis of the G1 poly(propylene thiophenoimine) (G1PPT) dendrimer was carried out by condensation reaction of PPI with 2-thiophene carboxaldehyde. A reaction mixture of poly(propylene imine) generation one dendrimer (1.65 g or 5.2 mmol) and 2-thiophene carboxaldehyde (2.34 g or 20.85 mmol) in a 50 mL dry methanol was stirred magnetically under a positive pressure of nitrogen gas for 2 days in a 100 mL three-necked round-bottom flask.

The removal of the methanol from the reaction mixture was done with rotatory evaporator and residual oil was dissolved in 50 mL dichloromethane (DCM), the organic phase was then washed with 50 mL of water 6 times to remove unreacted monomer. The DCM was removed by rotary evaporation so as to obtain the desired product as yellow oil. The method employed for this synthesis is a slight modification of that reported by Smith and his co-worker[22] and Salmon and Jutzi[23]. The yield of the thiophene functionalized dendrimer, poly(propylene thiophenoimine), shown in Scheme 1 was 1.56 g, 65%. The <sup>1</sup>H NMR (CDCl<sub>3</sub> 200 MHz, ppm) data for G1PPT are 1.34 (s, br, 4H, H-1), 1.74 (t, 8H, H-2), 2.42 (m, br, 12H, H-2&3), 3.51 (t, 8H), 6.90 (t, 8H, H-8), 7.01 (s, 4H, H-7), 7.23 (s, 4H, H-6), 7.8 (C<sub>4</sub>H<sub>3</sub>S). The G1PPT gave a new <sup>1</sup>H NMR of chemical shift at 8.30 ppm which is not shown in the parent G1PPI. Strong FTIR peak at 1632 cm<sup>-1</sup> which may be attributed to the formation of C = N bond in the dendrimer moiety while out of plane vibration for thiophene ring was obtained at 789 cm<sup>-1</sup> which correspond to earlier report[15, 24].

#### 2.4. Electrochemical preparation of generation 1 poly(propylene thiophenoimine)-co-poly(3,4 ethylene dioxothiophene) dendritic star copolymer modified gold electrode.

Prior to surface modification, the gold working electrode was polished to a mirror-like surface with alumina powder of sizes 1.0, 0.3 and 0.05  $\mu\text{m}$ , respectively. The electrode was immersed in piranha for 10 minutes for effective cleaning followed by sonication of the electrode in ethanol and water consecutively for 5 min. The electrode was further cleaned electrochemically in sulphuric acid by cycling between the potential of -200 mV to 1,500 mV until a reproducible cyclic voltammogram was obtained. Subsequently the gold electrode was rinsed with copious amount of water and absolute ethanol respectively. 6  $\mu\text{L}$  of 10 mg/mL of poly(propylene thiophenoimine)-(G1PPT) film was drop coated on the surface of the bare gold electrode for 12 h for effective self assembly of the film. The modified electrode was immersed into an aqueous solution of 0.1 M lithium perchlorate containing 0.1 M 3,4-ethylenedioxythiophene and 0.1 M sodium dodecyl sulphate by cycling the potential between -1,000 mV to 1,000 mV at a scan rate of 50 mV/s for ten cycles to obtain G1PPT-co-PEDOT film shown in fig 2. The same experimental procedure was used to prepare homopolymer onto the bare polished electrode with an exception of G1PPT on the electrode surface.



**Scheme 1.** Synthesis process

#### 2.5. Fabrication of the aptasensor.

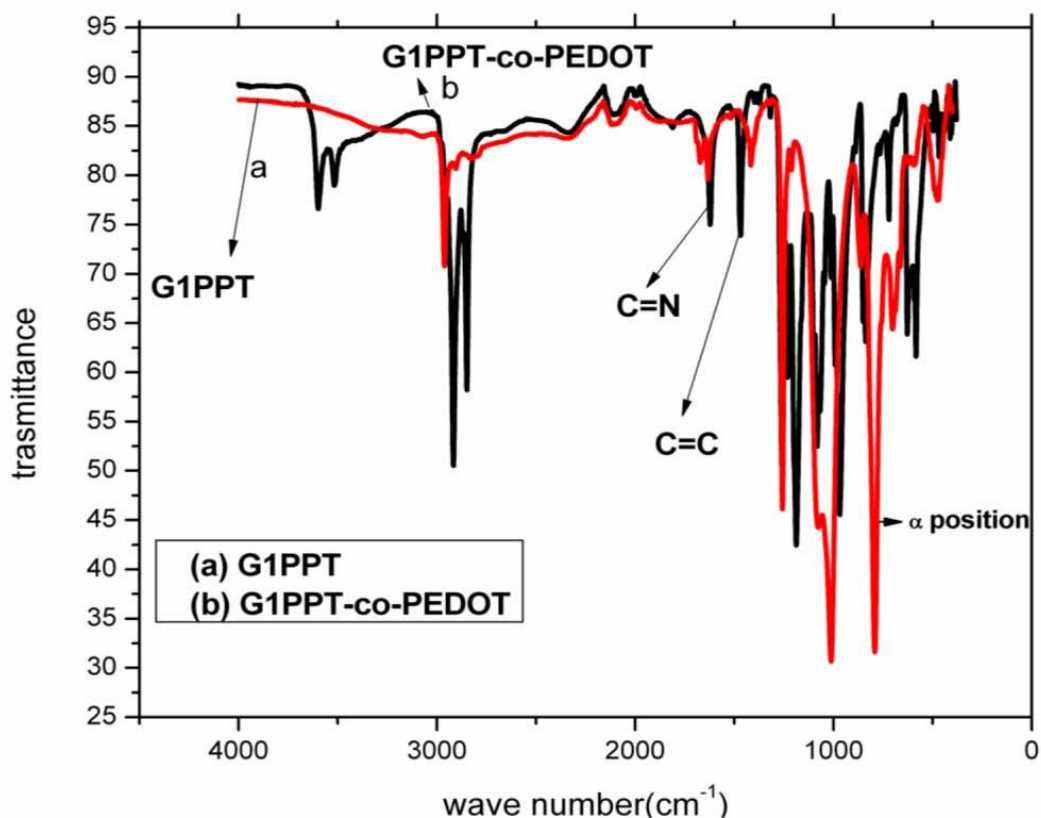
A self assembled monolayer of 3, 3' dithiodipropionic acid (DPA) on the G1PPT-co-PEDOT film modified electrode was formed by incubation in an ethanolic solution of 50 mM dithiodipropionic acid for 30 min. The unbound DPA was removed by washing the electrode in absolute ethanol and

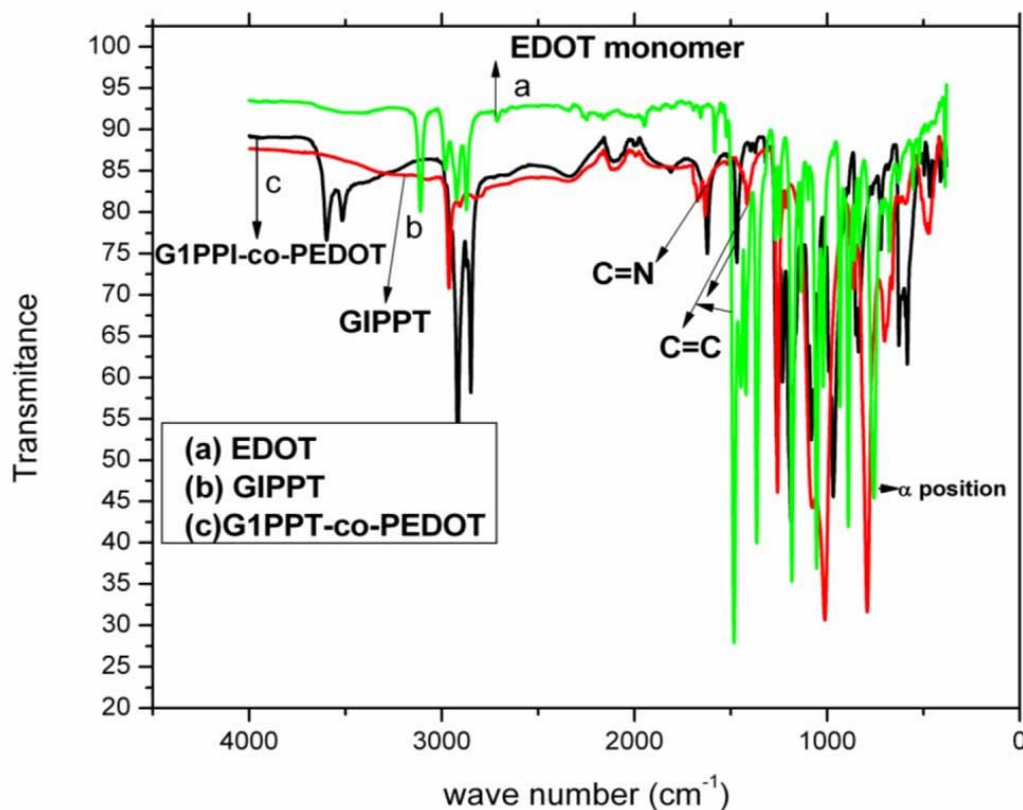
then Millipore water respectively. The DPA was activated by immersing the electrode in the same volume of 1 mM each of EDAC and NHS to activate the carboxylic group for easy bonding with the amine group of streptavidin for 60 min. The electrode was then functionalized with streptavidin by incubating in PBS (pH 7.5). solution containing 10  $\mu\text{g/mL}$  streptavidin for 60 min at 25  $^{\circ}\text{C}$  and was later rinsed in PBS The biotylated ssDNA aptamer was immobilized on the surface of the modified electrode via biotin- streptavidin interaction for 120 min at 25  $^{\circ}\text{C}$ . For the purpose of detection 10 nM aptamer was immobilized on the modified electrode surface. The Au|G1PPT-co-PEDOT |76-mer-ssDNA-Aptamer| electrode was incubated with different concentration of 17 $\beta$ -estradiol prepared in binding buffer.

### 3. RESULTS AND DISCUSSION

#### 3.1. Fourier transforms infrared spectroscopy (FTIR)

Thiophene monomer (EDOT), poly(propylene thiophenoimine) (G1PPT) dendrimer synthesized, homopolymer (PEDOT) and star copolymer (G1PPT-co-PEDOT) were analyzed with Fourier transform infra red spectroscopy (FTIR).The spectra of the thiophene monomer (EDOT) have several characteristic peaks at 387, 521, 631, 677, 758, 859, 933, 1054, 1099, 1135, 1183, 1271, 1468, 1583 and 2980  $\text{cm}^{-1}$ (fig1).





## B

**Figure 1.** Fourier transforms infrared spectra of spectroscopy of (A) G1PPT-co-PEDOT and G1PPT (B) FTIR spectra of EDOT monomer, G1PPT-co-PEDOT and G1PPT

Stretching vibration at 1468 and 1583  $\text{cm}^{-1}$  originate from the stretching modes of C=C, and 1099  $\text{cm}^{-1}$  from S-H of the thiophene ring. The C-H bending of thiophene can be observed at 1054  $\text{cm}^{-1}$  and 758  $\text{cm}^{-1}$ . In the spectrum of the functionalized dendrimers several characteristic peaks at 476, 720, 792, 862, 1012, 1258, 1213, 1417, 1633, 1672, 2120, 2917, 2962  $\text{cm}^{-1}$  for G1PPT were observed. The band at 2917 and 2962  $\text{cm}^{-1}$  in G1PPT indicate the presence of the  $\text{CH}_2$  stretching [15]. The sharp bands at 1632  $\text{cm}^{-1}$  is attributed to the C=N bond stretching vibration present in the dendrimer moiety. In the spectrum of the G1PPT out of plane bending of C-H bending located at the  $\alpha$ -position of the thiophene ring was observed at 720  $\text{cm}^{-1}$  [15].

The spectra of the star copolymer (G1PPT-co-PEDOT) and homopolymer (PEDOT) prepared by polymerization in 0.1 M  $\text{LiClO}_4$  containing 0.1 M sodium dodecyl sulphate (SDS) and 0.1M EDOT (monomer) showed several characteristics peaks at 627, 788, 837, 969, 1012, 1083, 1190, 1258, 1232, 1468, 1622, 2917, 2847, 2954  $\text{cm}^{-1}$  and 626, 769, 850, 980, 1108, 1131, 1199, 1376, 1405, 1474, 1497, 2920  $\text{cm}^{-1}$ , respectively. The band at 627, 1190 and 626, 1199  $\text{cm}^{-1}$  confirms the presence of perchlorate ion used as the dopant during polymerization [25]. In the spectrum of the G1PPT-co-PEDOT a band with a sharp peak for C=N in G1PPT-co-PEDOT now appears at 1622  $\text{cm}^{-1}$  but was completely absent in PEDOT spectrum. In addition, the absorbance at 720  $\text{cm}^{-1}$  completely disappears

after the polymerization, indicating that the G1PPT was converted to G1PPT-co-PEDOT via  $\alpha$ - $\alpha$  coupling of thiophene units. The band at 789 corresponds to C-H out of plane vibration in thiophene ring [15]. The vibration of C-S bond in the thiophene ring is revealed at  $837\text{ cm}^{-1}$  which is similar to earlier reports[15, 25] The FTIR spectrum are shown in (fig 1) below.

### 3.2. Fluorescence spectroscopy

To further confirm the formation of the functionalized dendrimer (G1PPT.), florescence ability of the functionalized dendrimer was investigated using fluorescence spectroscopy. The dendrimer (G1PP1) exhibited fluorescence properties with an excitation and emission band at 385 and 455 nm respectively for the dendrimer used in this work before functionalization compared to 390 and 450 reported earlier which may be attributed to aging [26] The functionalized dendrimer synthesized also exhibited fluorescence properties with a shift in excitation and emission wavelength to 381 and 480 nm respectively as shown in fig 3 which is similar to the earlier report [26]. In addition a Plasmon UV absorption of 295 nm was observed for G1PPT which was within the range of 250-400 nm reported for dendrimer functionalised with thiophene [15].

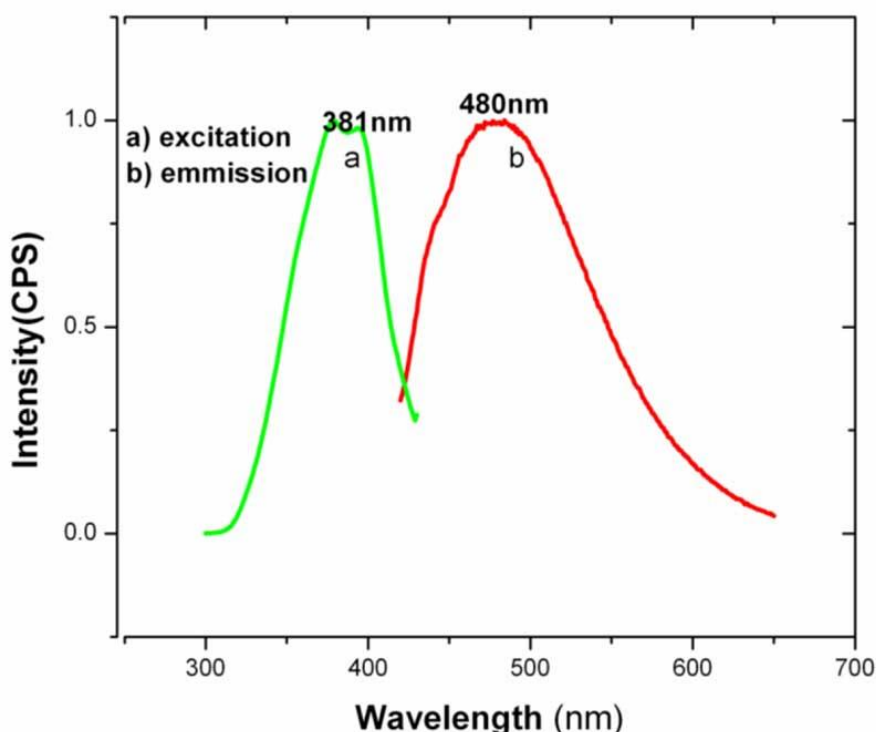


**Figure 2.** Excitation and emission spectra of the G1 poly(propylene thiophenoimine)-(G1PPT) dendrimer

Fig. 3a b and c shows the scanning electron micrograph of G1PPT., PEDOT and G1PPT-co-PEDOT electrode surface respectively. The morphology of the different synthesis' processes is presented in

fig 3 above. The morphology of the functionalized dendrimer revealed a homogeneous globular form on the electrode surface capable of undergoing growth compared to PEDOT film morphology that exhibited different appearance (flaky) with some small holes in between the flaky form which may allow the incorporation of the dendrimer. A significantly different morphology was observed for star copolymer (G1PPT-co-PEDOT) which may be attributed to the enlargement of the globular structures of the dendrimer moiety growing through the available holes in the PEDOT film which might be considered as further proof of copolymerization.

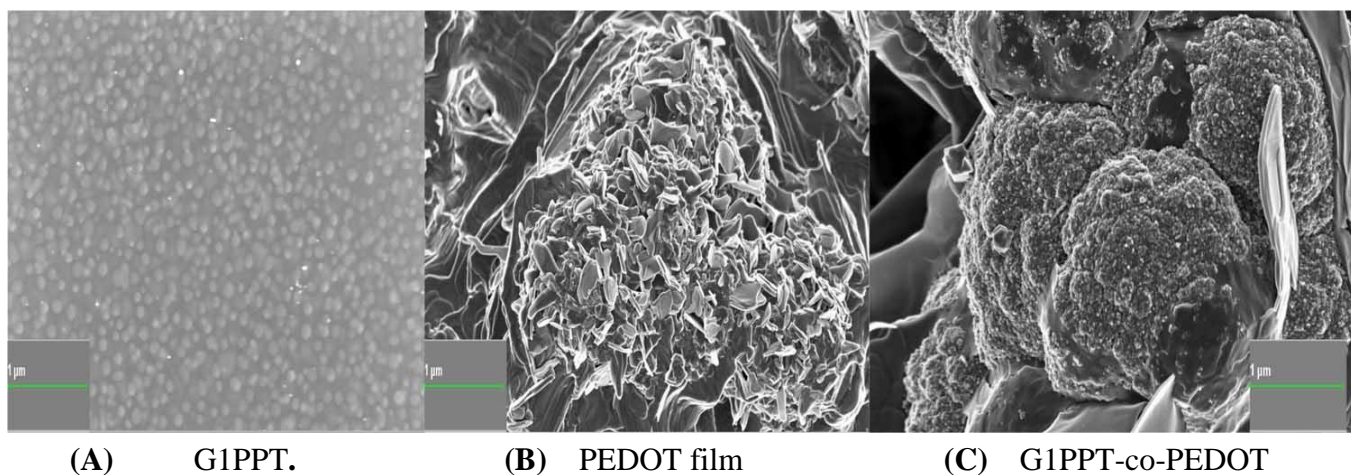


**Figure 3.** Scanning electron micrographs of (a) G1PPT (b) PEDOT (c) G1PPT-co-PEDOT gold electrode.

### 3.4. Cyclic voltammetric behavior of the modified electrode

Cyclic voltammetry is an effective and convenient tool to monitor the barrier of the modified electrode, because the electron transmission between the solution species and the electrode must occur by tunnelling either through the barrier or through the defects in the barrier. In this work the electrochemical behaviour of the stepwise fabrication process was studied in a pH 7.5 phosphate buffer saline containing 5 mM  $[\text{Fe}(\text{CN})_6]^{-3/4}$  serving as an electrochemical redox probe. The cyclic voltammogram of  $[\text{Fe}(\text{CN})_6]^{-3/4}$  at different modified electrode were illustrated in ( Fig 4).

A pair of well defined redox peaks was observed at the bare electrode (curve a) compared to the electrode modified with functionalised dendrimer which showed drastic decrease in peak currents (curve b).

This may be attributed to the compact nature of the functionalised film coated on the electrode which hindered the electron flow or the active probe channel from approaching the surface of the electrode as well as the SH linkage from the thiophene on the dendrimer to the gold electrode(S-Au linkage) which is negatively charge resulting in electrostatics repulsion with the negatively charged  $[\text{Fe}(\text{CN})_6]^{3/4}$  redox probe [14]. An increase in peak current was observed at (curve a) on modification of the electrode with PEDOT a conducting polymer (curve c) which accelerate the rate of electron transfer due to decrease in the electron transfer tunnelling between the probe and the electrode as result

of the electrostatic attraction between the positively charged backbone of the homopolymer and the negatively charged  $[\text{Fe}(\text{CN})_6]^{-3/-4}$  probe.

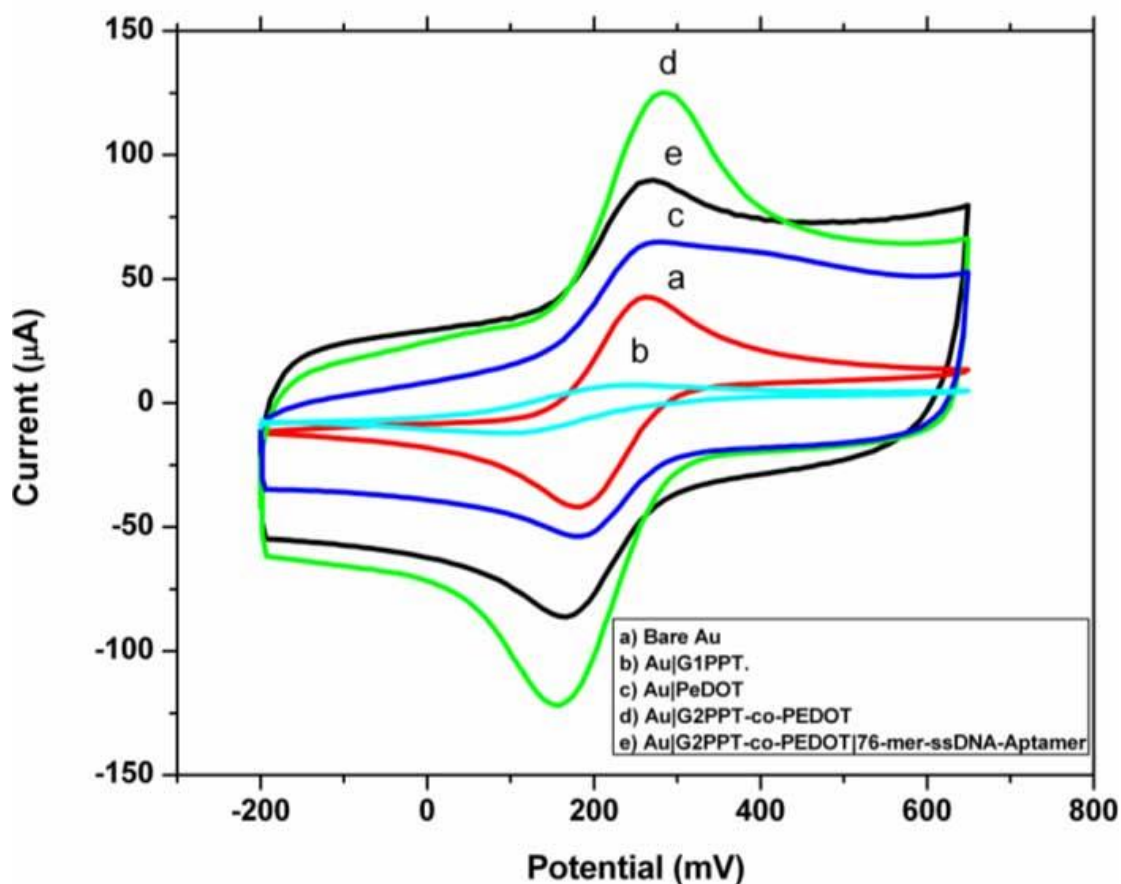


**Figure 4.** Cyclic voltammetry of modified electrode in 5 mM  $[\text{Fe}(\text{CN})_6]^{-3/-4}$  in phosphate buffer containing 0.1 M KCl at (a) Bare Au (b) Au|G1PPT| (c) Au|PEDOT|, (d) Au|G1PPT-co-PEDOT| (e) Au|G1PPT-co-PEDOT|76-mer-ssDNA-Aptamer|

A significant response change occurred compared to (curve c) after the functionalised dendrimer was copolymerized with PEDOT to form a star copolymer on the surface of the electrode which may be attributed to the combination of the unique properties exhibited by the functionalised macromolecule and the conducting polymer as well as the electrostatic attraction between the negatively charged redox probe and the positive charge backbone of the platform (G1PPT-co-PEDOT) which further decreases the electron transfer tunneling thereby increasing the rate of electron transfer to the surface of the electrode.

A slight decrease in peak current of probe  $[\text{Fe}(\text{CN})_6]^{-3/-4}$  ion on Au|G1PPT-co-PEDOT|76-mer-ssDNA-Aptamer| was observed at the aptamer modified electrode as compared to those obtained with the copolymer modified gold electrode, this also reflects the electrostatic repulsion that occurred between the negatively charged phosphate backbone of the ssDNA aptamer and the negatively charged

$[\text{Fe}(\text{CN})_6]^{3-/4}$  probe. The result of this modification shows that ssDNA aptamer was successfully attached to the star copolymer (G1PPT-co-PEDOT) modified gold electrode surface.

### 3.5. Electrochemical behaviour of the G1PPT-co-PEDOT (star copolymer) platform

The electrochemical behaviour of the star copolymer was investigated using cyclic voltammetry. of the star copolymer consisting of functionalized dendrimer copolymerized with PEDOT. G1PPT-co-PEDOT at different scan rates in  $[\text{Fe}(\text{CN})_6]^{3-/4}$  as a redox probe, showed an increase in peak current as the scan rate increases which illustrate the presences of immobilized electroactive copolymer layer at the electrode with no shift in the peak potential (Fig. 5). A linear dependence of anodic current on the scan rate was observed when a plot of  $i_{pa}$  versus scan rate was done with a correlation coefficient of 0.991. It can thus be deduced that the platform is a characteristic of surface-bound thin film electroactive species undergoing fast electron transfer reaction at the electrode. The rate of electron transport on the copolymer (that is diffusion coefficient of the electron ( $D_e$ )) was calculated to be  $4.50 \times 10^{-7} \text{ cm}^2 \text{ s}^{-1}$  using Randle Sevcik equation,

$$I_p = 2.69 \times 10^5 n^{3/2} A D^{1/2} \nu^{1/2} C \quad (1)$$

where  $I_p$  = peak current  $n$  = number of electron transfer,  $A$  = area of an electrode,  $D_e$  = diffusion coefficient and  $\nu$  = scan rate  $C$  = concentration of bulk solution.

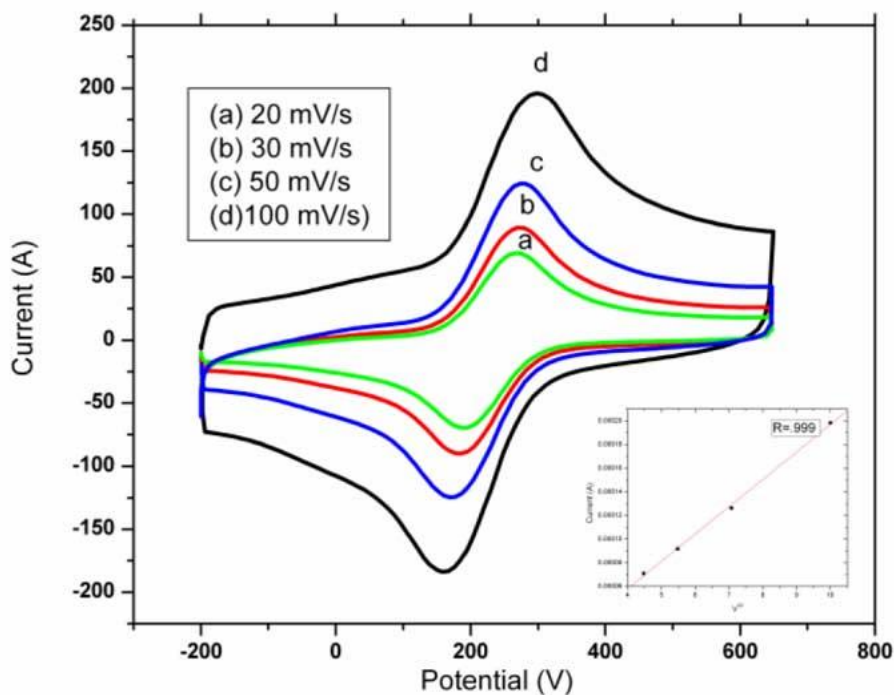


**Figure 5.** Cyclic voltammetry of star copolymer Au|G1PPT-co-PEDOT at different sweep rates at (a) 20 mV/s (b) 30 mV/s (c) 50 mV/s (d) 100 mV/s in 5 mM  $[\text{Fe}(\text{CN})_6]^{3-/4}$  redox probe in PBS containing 0.1 M KCl.

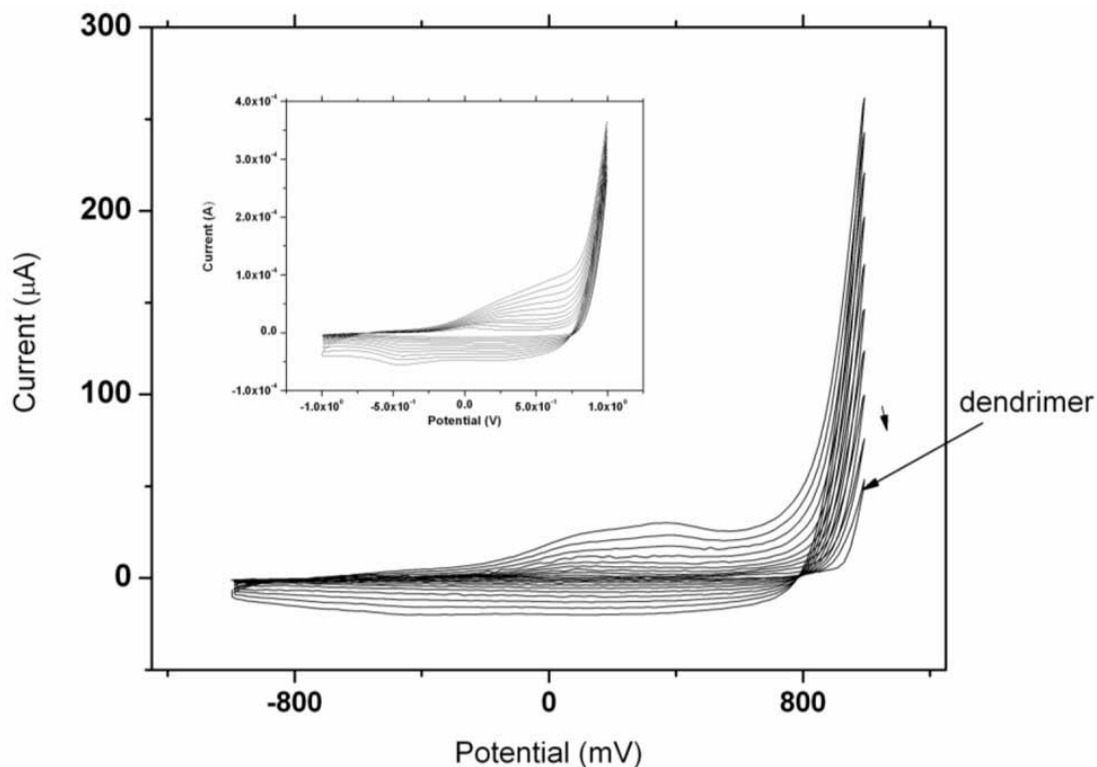


**Figure 6.** Electropolymerization of functionalized dendrimer (G1PPT) in 0.1 M lithium perchlorate containing 0.1 M EDOT and 0.1 M SDS at a scan rate of 50 mV/s with (PEDOT film insert)

The obtained value is high compared to  $2.20 \times 10^{-8} \text{ cm}^2 \text{ s}^{-1}$  for bare. The high value may be attributed to the formation of the copolymer on the surface of the electrode which showed a facile flow of electron due to the combination of the unique properties of the macromolecule (dendrimer) and the conducting polymer (PEDOT) (scheme 2) which resulted in an increase in conductivity of the G1PPT-co-PEDOT copolymer due to increase in the conjugation length resulting in a  $D_e$  value approximately one order of magnitude higher than bare and PANI doped with poly vinyl reported earlier [27]. The reproducibility of the G1PPT-co-PEDOT was investigated with cyclic voltammetry. The platform exhibited reversible electrochemistry in  $[\text{Fe}(\text{CN})_6]^{-3/4}$  with formal potential of  $230 \pm 10 \text{ mV}$  for six different measurements demonstrating the good reproducibility of the platform.

### 3.6. Electrosynthesis of the G1PPT-co-PEDOT star copolymer

A G1PPT-co-PEDOT composite film modified electrode was fabricated by electropolymerization of 3, 4-ethylenedioxythiophene (EDOT) in the presence of G1PPT drop coated on a gold electrode.

The experiment were performed in 0.1 M lithium perchlorate containing 0.1 M sodium dodecyl sulphate with cyclic voltammetric sweep in the potential range of -1,000 mV to 1,000 mV at scan rate of 50 mV/s. The cyclic voltammogram of EDOT with or without G1PPT were compared in fig 6. One of the primary differences between the two polymerization processes is the change in current response.

A slight drop in current was observed in the presence of G1PPT compared to electropolymerization in the absence of the functionalized dendrimer. An oxidation peak associated with G1PPT is apparent at 995 mV with no increase in current as expected for the film growth which revealed electrodeposition of dendrimer on the surface of the electrode [28]. A shoulder corresponding to the oxidation potential of EDOT is present at 986 mV.

The oxidation and reduction peak potential of the copolymer G1PPT-co-PEDOT was observed at 230 mV and -490 mV respectively compared to PEDOT film which was obtained at 290 mV and -603 mV respectively. The oxidation potential shifted to less positive value which is an indication of the formation of copolymer [25]. An irreversible electro oxidation of 1330 mV for functionalised dendrimer (G4PPI-2Th) has been reported earlier [29].

The change in oxidation and reduction peaks may be attributed to the formation of the copolymer. Copolymers have been reported to decrease the onset of oxidation, which can successfully prevent overoxidation [25, 30]. The decrease in the onset of oxidation can as well be linked to the generation of dendrimer employed for this work as well as the type of electrolytes. As shown in fig.6 the film obtained for G1PPT-co-PEDOT is quite different from the PEDOT film which could serve as indication to copolymer formation.

### *3.7. Electrochemical characterization of the G1PPT-co-PEDOT film modified on gold electrode in supporting electrolyte*

The copolymer film obtained by electropolymerization process was characterized by cyclic voltammetry at scan rates between 30 and 100 mV/s in a monomer free 0.1M LiClO<sub>4</sub>. The corresponding cyclic voltammogram presented in fig 7 shows a linear dependence of the peak current with scan rate, which is a characteristic of surface-bound copolymer thin film electroactive species undergoing fast electron transfer reaction at the electrode with electrons diffusion taking place along the copolymer chain. It is interesting to note that the film exhibits a relatively broad but reversible redox process which illustrates its electroactivity.

The two redox couples were observed at a lower potential of 230 mV and -490 mV compared to what was obtained for PEDOT film, thereby confirming the formation of a copolymer [30]. The existence of this redox couples is an indication that the redox chemistry mechanism may involve cation and anion diffusing in and out of the film.

The redox chemistry of the copolymer involves ion transport in and out of the film (insertion and removal) in the electrolytes. The anodic and cathodic waves could be explained by incorporation of a counter- ion. The ClO<sub>4</sub><sup>-</sup> anion incorporated into the copolymer matrix would interact with the oxidation site of the film as counter ion. The electronic rearrangement of the redox reaction process (oxidation and reduction process) involving the removal and incorporation of the counter ion forms a conducting polycation in the presence of the charge-balancing anion as shown in scheme 2 .The first redox couple ( $i_{pa1}$  and  $i_{pc1}$ ) can be attributed to the introduction and release of the Li<sup>+</sup> cation while the other redox couple ( $i_{pa2}$  and  $i_{pc2}$ ) correspond to the insertion and release of the ClO<sub>4</sub><sup>-</sup> anions respectively.

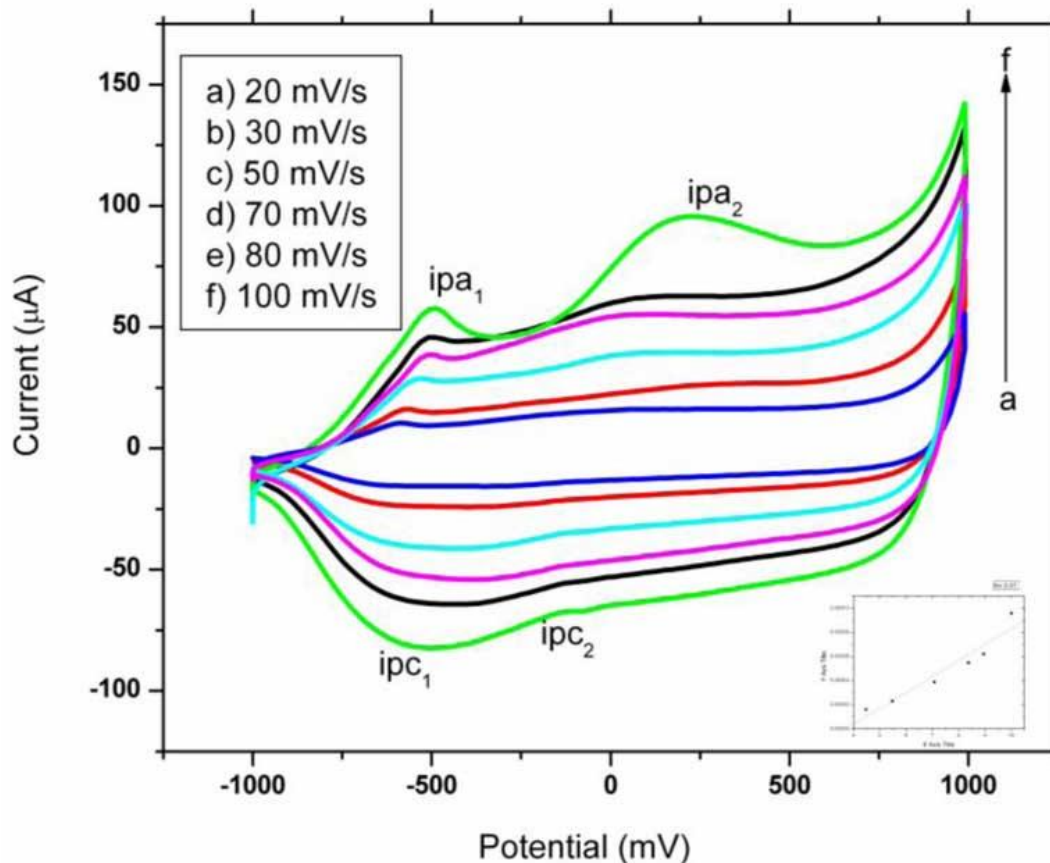
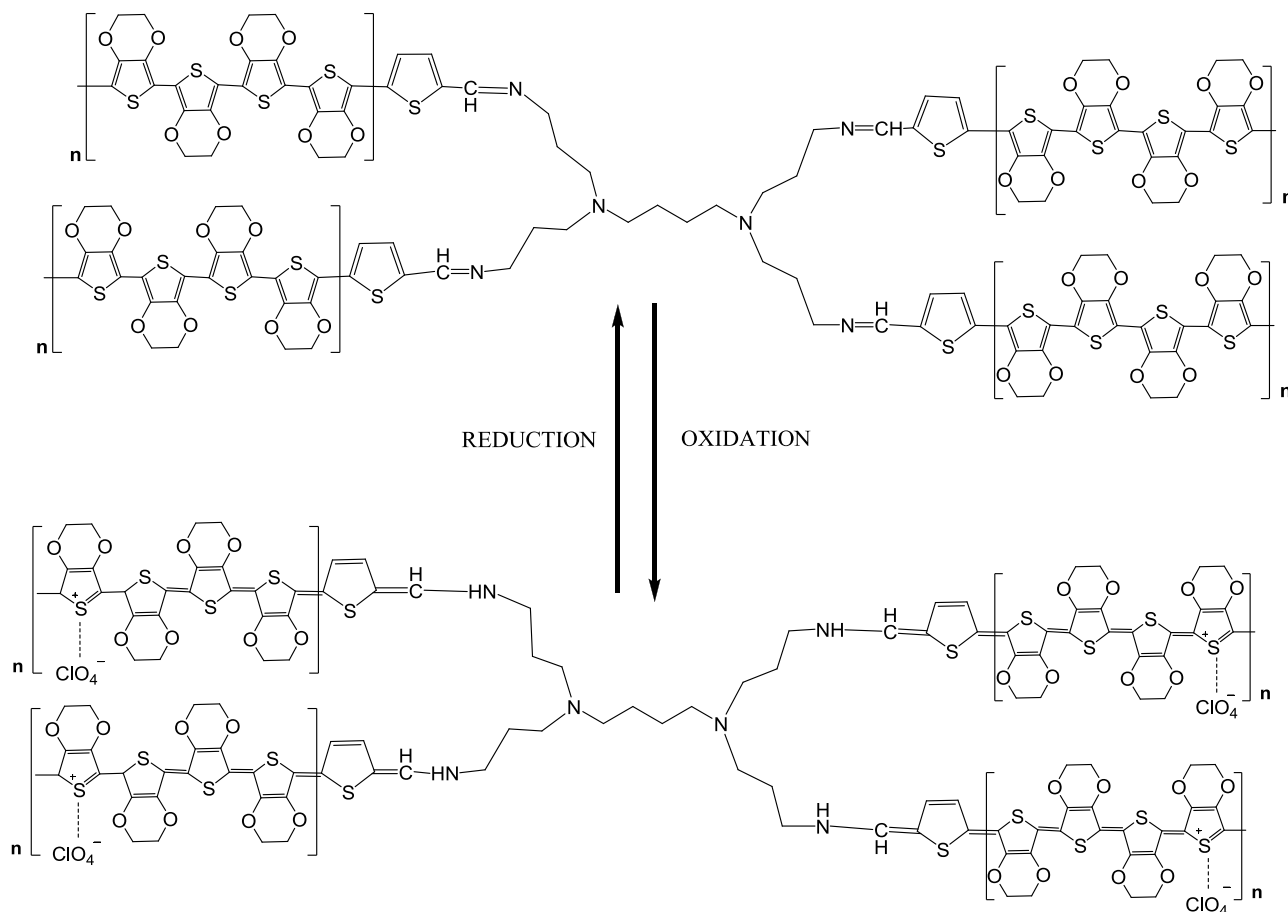


**Figure 7.** Characterization of the Au|GIPPT-co-PEDOT| film modified on gold electrode in 0.1 M monomer free lithium perchlorate at scan rates of (a) 20 mV/s; (b) 30 mV/s; (c) 50 mV/s; (d) 70 mV/s; (e) 80 mV/s; (f) 100 mV/s.

### 3.8. Electrochemical impedance spectroscopy (EIS) characterization of GIPPT-co-PEDOT film modified electrode.

Electrochemical impedance is an effective tool for studying the interfacial properties of surface modified electrode. The impedance characteristics of any electrode system depends on the overall effect of several parameters which include electrolyte resistance ( $R_s$ ), charge transfer resistance ( $R_{ct}$ ) between the solution and the electrode surface, Warburg element ( $Z_w$ ) and double layer capacitance ( $C_{dl}$ ) (due to the interface between the electrode surface and the solution). The use of a constant phase element instead of the capacitance is required to optimize the fit to the experiment and this is due to the nonideal nature of the electrode [31-32].

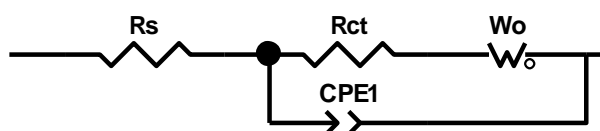
The complex impedance can be described as the sum of the real ( $Z_{rel}$ ) and the imaginary ( $Z_w$ ) component that originate from the resistance and capacitance of the cell. Furthermore, for the purpose of giving additional detailed information about impedance of the modified electrode, a modified Randles equivalent circuit fitting was chosen to fit the measured results.



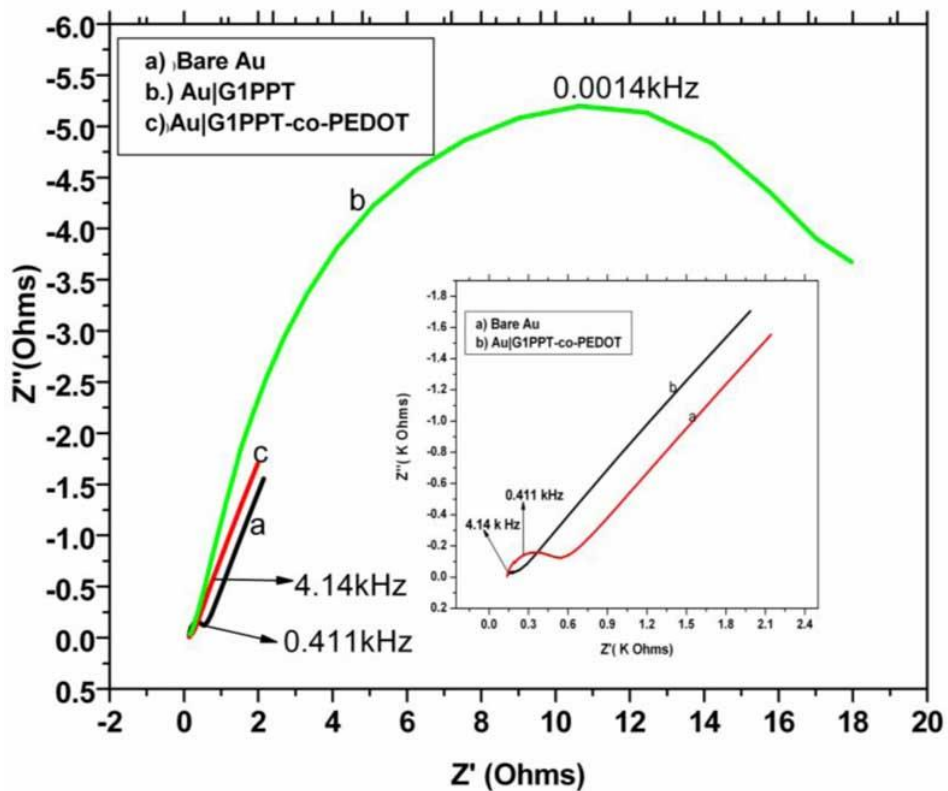
**Scheme 2.** The redox process mechanisms

The two components in the circuit,  $R_s$  and  $Z_w$  correspond to bulk properties of the electrolyte solution and the diffusion of the probe applied respectively. These two components are not affected by chemical change occurring at the surface of the electrode.  $C_{dl}$  and  $R_{ct}$  which are the components of the circuit depend on dielectric and the insulating features at the electrode/electrolyte interface. However among them all  $R_{ct}$  is the most directive and sensitive parameter that respond to change on the electrode interface. In EIS the semicircle diameter corresponds to the charge transfer which varies on modification of the electrodes.

The electrochemical impedance measurements were carried out in a background solution of 5 mM  $Fe(CN)_6^{3-/4-}$  PBS (0.1 M, pH 7.5) at a bias potential of 224 mV. The alternative current of 10 mV and the frequency of  $10^{-1}$ - $10^6$  Hz were applied. The results of the Faradaic impedance data for bare Au, Au|G1PPT and Au| G1PPT-co-PEDOT | are shown in (fig 8) (inset contains data for bare Au and Au| G1PPT-co-PEDOT |). Significant different in  $R_{ct}$  values were observed upon modification of the



(A)



(B)

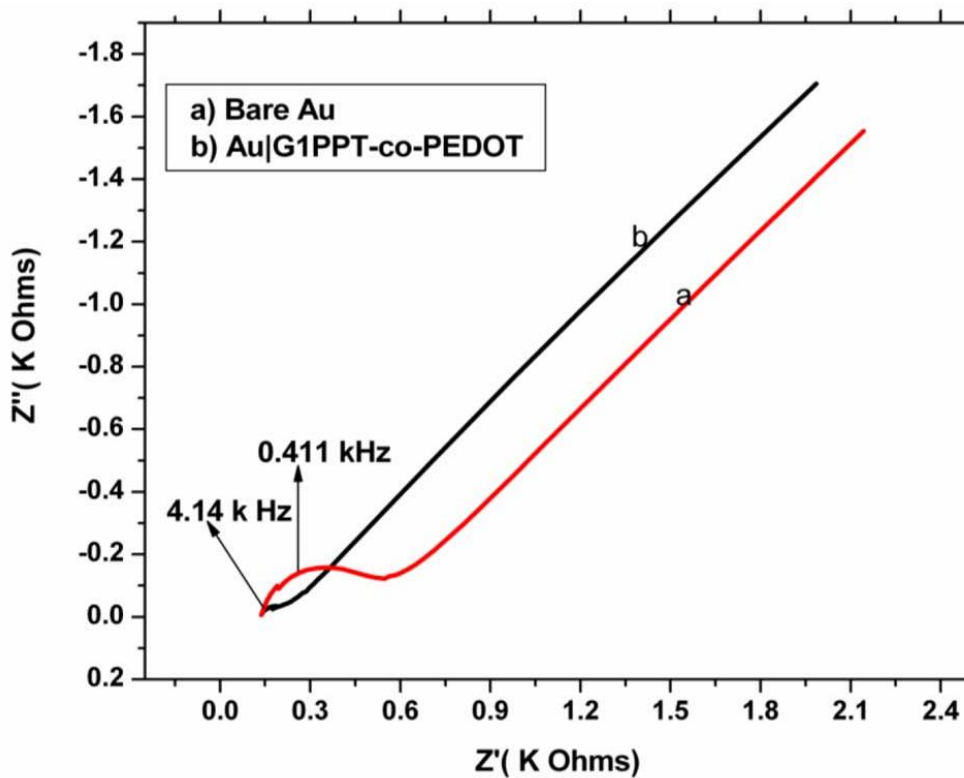
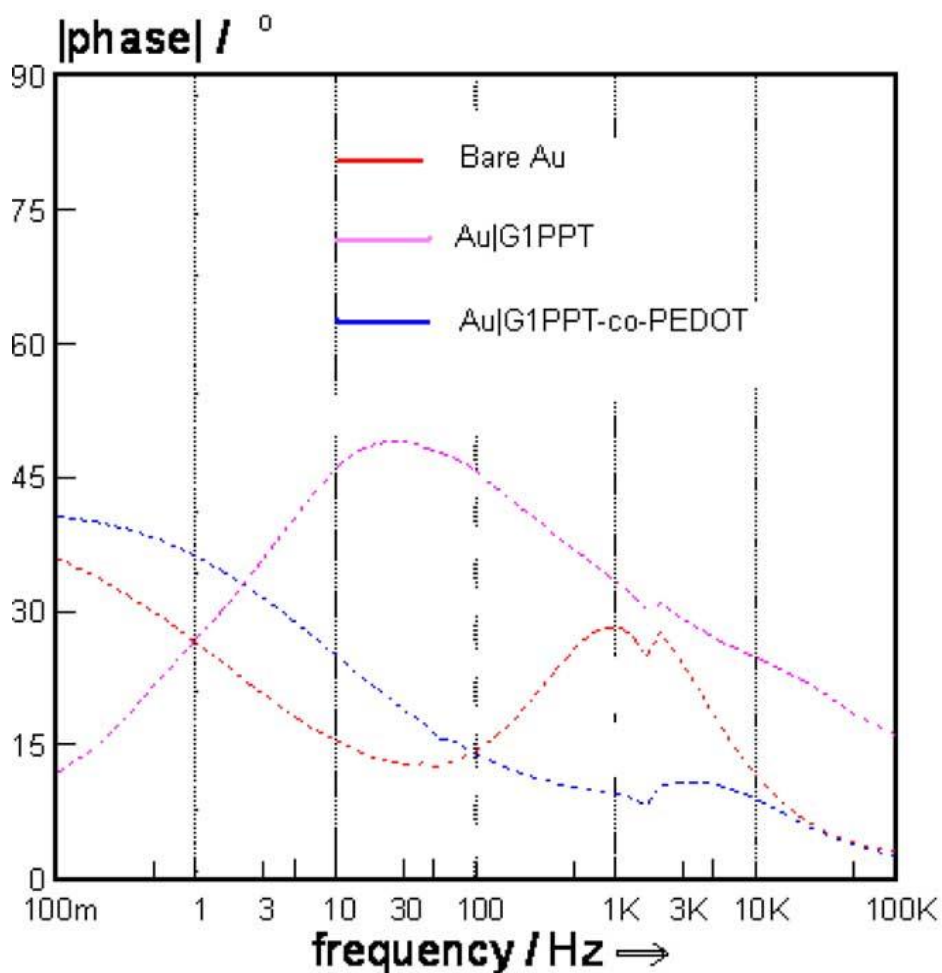


**Figure 8B (insert).** Nyquist (a) Au|, ( b) Au| G1PPT-co-PEDOT | in  $\text{Fe}(\text{CN})_6^{3-/4-}$  redox probe at 224 mV.



(C) Bode plots

**Figure 8.** (A) Randle equivalent circuit (B) Nyquist and (C) Bode plots of (a) Au|, (b) Au|G1PPT| and (c) Au|G1PPT-co-PEDOT| in  $\text{Fe}(\text{CN})_6^{3-/4-}$  redox probe at 22mV

electrode. It can be seen from fig 8 that the bare electrode exhibited a small semicircle domain which corresponds to  $R_{ct}$  value of approximately  $3.962 \times 10^2 \Omega$ . The  $R_{ct}$  increased remarkably to  $17.795 \times 10^3 \Omega$  upon the formation of the first interface of the G1PPT film (fig 8b), which indicated that the compact film acts as a definite kinetic barrier for the electron transfer from the functionalized dendrimer to the transducer. On modification of the electrode with G1PPT-co-PEDOT a tremendous decrease in  $R_{ct}$  to  $9.0 \times 10^1 \Omega$  was observed which resulted in an almost straight line which is characteristic of diffusion limiting step due to the extremely fast electron transfer process. This is attributed to the electrostatic attraction between the cationic backbone of the copolymer platform and negatively charged  $\text{Fe}(\text{CN})_6^{3-/4-}$  redox probe. The decrease in  $R_{ct}$  was found to be 99.6 % compared to the electrode modified with G1PPT alone which may be attributed to the combination of the unique properties exhibited by the dendrimer and conducting polymer films which played an important role in accelerating the electron transfer by reducing the electron transfer tunneling as well as their high compatibility suggesting an improved conductivity of the star copolymer (G1PPT-co-PEDOT) platform.

An investigation into the catalytic behaviour of the platform was carried out with an estimation of some useful kinetic parameters such as time constant ( $\tau$ ), exchange current ( $i_o$ ) heterogeneous rate constant ( $k_{et}$ ) to determine the effect of the platform on the kinetics of the Fe (CN)<sub>6</sub>]<sup>-3/4</sup> redox probe [28, 33]. The kinetic parameters were calculated from equation 2a, 2b, 2c and 2d respectively.

$$w_{\max} = \frac{1}{R_{ct} C_{dl}} \quad (2a)$$

$$\tau = R_{ct} \times C_{dl} \quad (2b)$$

$$i_o = \frac{RT}{nFR_{ct}} \quad (2c)$$

$$i_o = nFAK_{et}C^* \quad (2d)$$

where  $w_{\max}$  (frequency at the max. imaginary impedance of the semicircle) =  $2\pi f$

$C_{dl}$  = double layer capacitance,  $C^*$  = bulk concentration of the redox probe,  $A$  = area of the electrode,

$R_{ct}$  = charge transfer resistance,  $n$  = no of electron and  $F$  = Faraday constant.

The values obtained for the exchange current at the bare Au and Au|G1PPT-co-PEDOT| platforms for the electron transfer process (table 1) are  $6.50 \times 10^{-5}$  A and  $2.83 \times 10^{-4}$  A, respectively. The estimated values revealed a fast electron transfer at the copolymer modified electrode than the bare electrode only.

The catalytic behaviour of this platform may be attributed to the increase in the influx of the Fe (CN)<sub>6</sub>]<sup>-3/4</sup> redox probe to the surface of the electrode as well as the electrostatic interaction that existed between the cationic copolymer back bone and the anionic redox probe [34]. Heterogeneous rate constant is a measure of the rate of electron transfer on the surface of the electrode, thus, an increase in the heterogeneous rate constant at the modified electrode also corroborated the facile flow of electron at the copolymer platform. In addition the time constant obtained at the copolymer platform was lower than on the bare electrode which is in agreement with earlier reports for modified electrodes [28].

**Table 1.** Kinetic parameters of aptamer sensor systems.

Kinetic parameters	Au	Au G1PPT	Au G1PPT-co-PEDOT
$w_{\max}$ (rads <sup>-1</sup> )	2633.	8.797	625789.54
Exchange current ( $i_o$ , A)	$6.50 \times 10^{-5}$	$1.44 \times 10^{-6}$	$2.83 \times 10^{-4}$
Heterogeneous rate constant ( $k_{et}$ , s <sup>-1</sup> )	$6.67 \times 10^{-3}$	$1.49 \times 10^{-4}$	$2.29 \times 10^{-2}$
Time constant ( $\tau$ , s rad <sup>-1</sup> )	$3.80 \times 10^{-4}$	$1.14 \times 10^{-1}$	$3.90 \times 10^{-5}$

The impedance parameters in table 1 were obtained by fitting the inset equivalent circuit and the fitting error were less than 5 %. The calculated parameters are given in table 1.

Surface coverage of 82% was obtained for the copolymer on the electrode which account for the high amount of aptamers that can be immobilized on the surface of the copolymer platform. The value was estimated from the  $R_{ct}$  value using the formula [28].

$$\theta = 1 - \frac{R_{ct} \text{ of modified electrode}}{R_{ct} \text{ of bare electrode}} \quad 3$$

From the Bode plot improved conductivity of the G1PPT-co-PEDOT modified electrode over bare gold electrode can be observed by the marked reduction in the impedance with phase angle shift.

### 3.9. Electrochemical detection of 17- $\beta$ -estradiol

An electrochemical aptamer based biosensor for the detection of 17 $\beta$ -estradiol an endocrine disruptor was developed. This electrochemical aptamer based biosensor was made up of a biotylated DNA aptamer immobilized on a gold electrode modified with a star copolymer (G1PPT-co-PEDOT). The analytical performance of the aptasensor was carried out by incubating different concentration of the 17 $\beta$ -estradiol with the immobilized aptamers. Electrochemical signals were recorded by cyclic voltammetry and square wave voltammetry which was done against a series of 17 $\beta$ -estradiol concentration (0.1 nM-100 nM) to probe the binding ability of the target with the aptamer immobilized on the platform. The analysis was done in the presence of a redox probe  $[\text{Fe}(\text{CN})_6]^{3-4}$  by monitoring the reduction in the electron flux produced from a redox reaction between the redox couple. In principle without the interaction between the aptamer probe and the target (17- $\beta$ -estradiol) a high peak current is expected. The interaction of the aptamer-target complex was monitored by change in peak current as the concentration of the target increases. Concentration dependence decrease in current signal was observed in CV and SWV. The decrease in signal response on incubation of the target with probe was achieved which may be attributed to specific interaction between the aptamer and 17 $\beta$ -estradiol ( $E_2$ ) which result in the formation of aptamer-target complex [35-36]. The formation of the aptamer-17 $\beta$ -estradiol complex on the electrode surface hindered the effective transfer of electron between the electrolyte solution (redox couple) and the electrode surface [36]. In addition it is well documented that aptamer undergo conformational changes upon binding their target. When 17 $\beta$ -estradiol as a specific competitor appears, 17 $\beta$ -estradiol-aptamer complex are formed rather than the aptamer DNA-duplex thereby increasing the electron transfer tunnelling between the redox probe and the electrode [37]. The aptamer-target complex insulates the electron transfer between the electrode surface and the electrolyte solution. Furthermore, the decrease in current can be attributed to the electrostatic repulsion that occur between negatively charge phosphate backbone and the negatively charge hydroxyl ion ( $\text{OH}^-$ ) of the target in solution due to it specific interaction with the aptamer. Though it has been reported that 17 $\beta$ -estradiol ( $E_2$ ) becomes negatively charge in solution due to the formation of more hydroxyl radical ion at high pH [38]. The changes in current ( $\Delta I$ ) observed for the

interaction of aptamer-target response were about 10-47% when  $17\beta$ -estradiol ( $E_2$ ) concentration was between 0.1-100 nM. It is evident that at higher concentration of  $17\beta$ -estradiol ( $E_2$ ), the current decreases more significantly which may be attributed to the formation of more hydroxyl ion of the estradiol in solution which prevented the influx of electron from the electrolyte to the surface of the electrode due to repulsion as a result of similar charges [36]. The difference in peak potential increased as the concentration of  $17\beta$ -estradiol increased. The increase in peak current separation may be attributed to slow kinetic of charge transfer electron which is caused by aptamer-target complex formation. The aptasensor is sensitive which may be attributed to the high surface coverage exhibited by the nanoelectrode which significantly enhanced the loading of the 76-mer-ssDNA-aptamer and hence markedly improve the sensitivity for the target.

A linear relationship between the log of concentration of the target and change in current was obtained with  $R = 0.989$  and the dynamic range was determined to be in the range of 0.1 – 100 nM of  $17\beta$ -estradiol ( $E_2$ ). A good reproducibility with a standard deviation of less than 5% was obtained ( $n = 6$ ) for the aptasensor. The fabricated aptasensor was found to retain 75% of its original response after it was stored in the refrigerator at  $4\text{ }^\circ\text{C}$  for half a month.

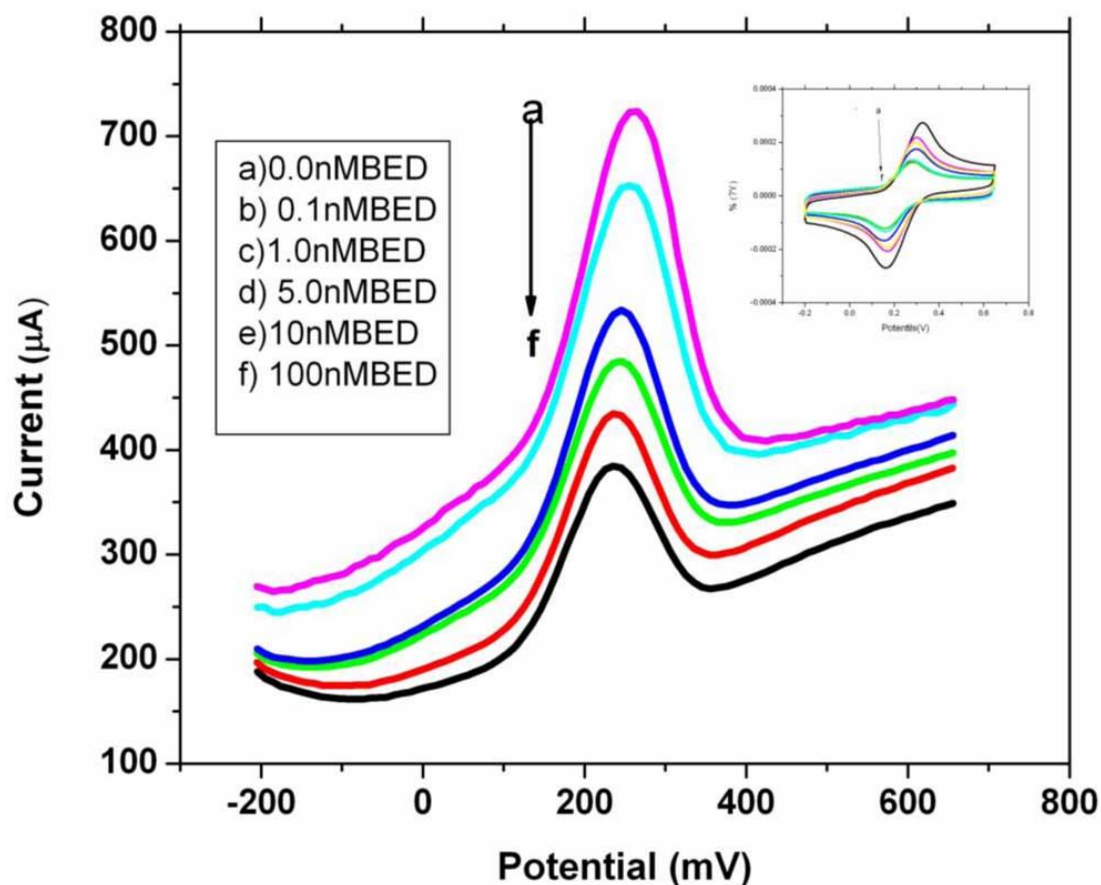


**Figure 9.** Electrochemical analysis of  $17\beta$ -estradiol ( $E_2$ ) using aptamer immobilized star copolymer (G1PPT-co-PEDOT) at different concentration (0.1-100 nM) with Square wave voltammogram in  $\text{Fe}(\text{CN})_6^{3-/4-}$ .

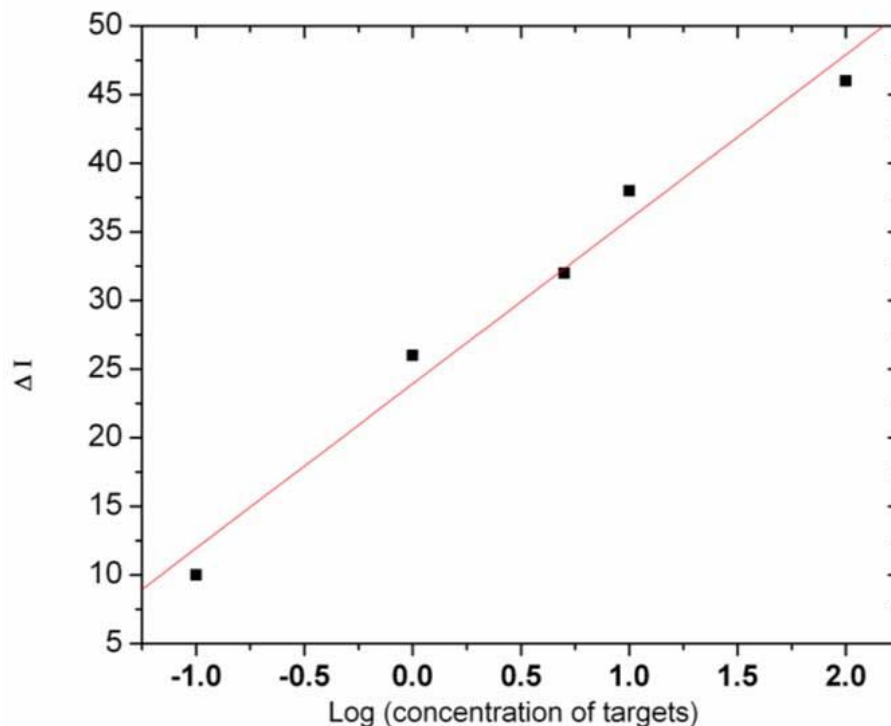


**Figure9 (a).**The linear relationship between the change in current and the log 17β-estradiol concentration. The regression equation was  $Y = 23.92687 + 11.99 \log X$  with a correlation coefficient of 0.989, where Y and X represent relative current response and the 17β-estradiol concentration respectively.

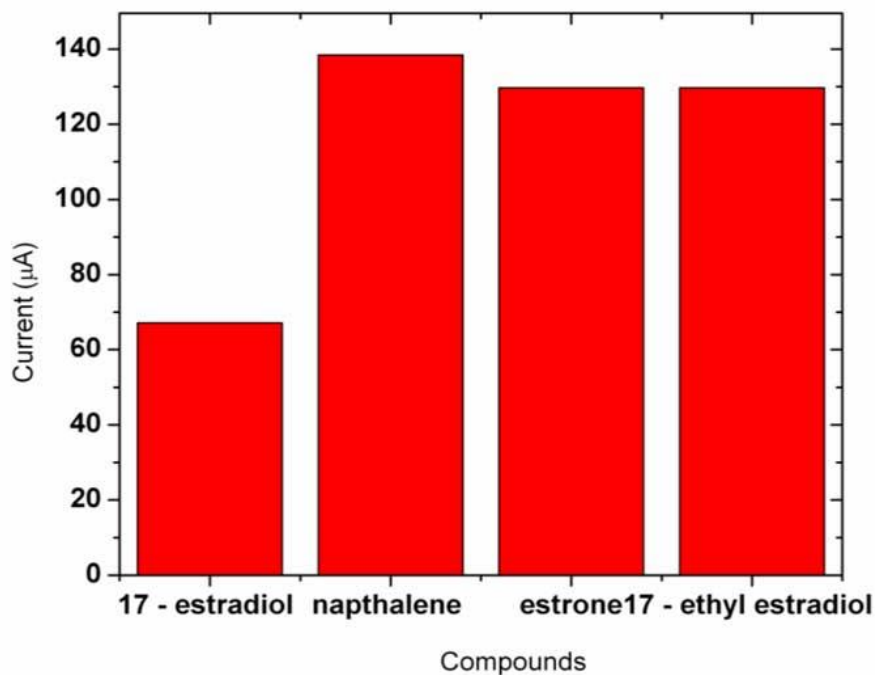


**Figure 10.** Current response of  $[Fe(CN)_6]^{3-/4-}$  probe in the presence of DNA aptamer to 10 nM 17α-ethynlestradiol, estrone, naphthalene and 17β-estradiol respectively.

### 3.10. Specificity of electrochemical aptamer based biosensor to 17 $\beta$ -estradiol ( $E_2$ )

Not only does an aptamer based biosensor have to be sensitive to different concentrations of the analyte, but also it must be specific. Experiments were thus conducted on 17 $\beta$ -estradiol, estrone, naphthalene and 17 $\alpha$ -ethylestradiol which belong to the family of endocrine disrupting chemicals. They were employed as control to assess the specificity of the aptasensor for the determination of 17 $\beta$ -estradiol. When the aptasensor was incubated with 10 nM estrone, naphthalene and 17 $\alpha$ -ethylestradiol respectively little or no significant change was seen in the SWV current response compared to the target due to lack of specific binding. A significant decrease induced by interaction of the aptamer probe and 17 $\beta$ -estradiol was observed due to high specific binding that occurred between 17 $\beta$ -estradiol and the aptamer probe which resulted in the insulation of the electron transfer between the electrode and the redox probe. The specificity of the aptamer toward the target may be based mostly on the change in the position of or absence of the minor functional group (OH<sup>-</sup>) in the molecule which is one of the subtle atoms specific for aptamer binding as well as the ability of the biological recognition element (aptamer probe) immobilized on the copolymer modified electrode to retained its unique ability to interact specifically.

## 4. CONCLUSION

A star copolymer G1PPT-co-PEDOT has been synthesized electrochemically and this was employed as a platform for the immobilization of 76-mer-ssDNA-aptamer to develop an electrochemical method for the detection of 17 $\beta$ -estradiol, an endocrine disrupting compound. The aptasensor showed higher specificity for 17 $\beta$ -estradiol when compared with the response to compounds having similar structure to 17 $\beta$ -estradiol such as naphthalene, estrone and 17 $\alpha$ -ethylestradiol.

## ACKNOWLEDGEMENTS

The research work was funded by the National Research Fund South Africa. We wish to thank the University of the Western Cape for the opportunity given to embark upon this research work.

## References

1. G.-C. Zhao, X. Yang, *Electrochem Commun*, 12 (2010) 300.
2. Q.Z. Neumann, Dongmao ; Tam , Felicia; Lal, Surbhi; Wittung-Stafshede , Pernilla; Halas, Naomi J., *Anal. Chem.*, 81 (2009) 10002.
3. S. Tombelli, M. Minunni, M. Mascini, *Biosenson and Bioelectron*, 20 (2005) 2424.
4. J.E. Smith , C.D. Medley, Z. Tang, D. Shangguan, C. Lofton , W. Tan *Anal. Chem.*, 79 (2007) 3075.
5. C. Pan, G. Manli., Z. Nie, X. Xiao, S. Yao, *Electroanalysis*, 21 (2009) 1321.
6. Z. Liu, R. Yuan, Y. Chai , Y. Zhuo, C. Hong, X. Yang, H. Su, X. Qian, *Electrochim Acta*, 54 (2009) 6207. L. Xiaoxia , Q. Honglan , S. Lihua, G. Qiang , Z. Chengxiao, *Electroanal*, 20 (2008) 1475.
7. W. Jianlong , W. Fuan, D. Shaojun, *J of Electroanal Chem*. 626 (2009) 1.

8. L. Fabien, A.H. Hoang, L. Mario, *Anal. Chem.*, 78 (2006) 4727.
9. D. Yan , L. Bingling, W. Hui, W. Yuling, W. Erkang, *Anal. Chem.*, 80 (2008) 5110.
10. Z. Zhang, W. Yang, J. Wang, C. Yang, F. Yang, X. Yang, *Talanta*, 78 (2009) 1240.
11. B. Klarjnert , M. Bryswewska, *Acta Biochimica Pol.*, 48 (2001) 199.
12. Thabile Ndlovu, Omotayo A. Arotiba, Rui W. Krause, B.B. Mamba, *Int. J. Electrochem. Sci.*, 5 (2010) 1179
13. G. Li, X. Li, J. Wan, S. Zhang, *Biosenson and Bioelectron*, 24 (2009) 3281.
14. Deng S., Locklin J., Patton D. , Baba A., Advincula R C., *J Am Chem Soc*, 127 (2005) 1744.
15. P.R.L. Malenfant, J.M.J. Frechet *Macromolecules*, 33 (2000) 3634.
16. J.J. Amaral Mendes *Food and Chem. Toxicol.*, 40 (2002) 781.
17. C.J. Koester, S.C. Simoni, B.K. Esser, *Anal Chem*, 75 (2003) 2813.
18. H. Kuramitz, M. Matsuda, J. Thomas , K. H;Sugawara , S. Tanaka, *The Analyst*, 128 (2002) 182.
19. Song J C, J. Yang , X.M. Hu, *J.Appl. Electrochem* 38: (2008) 833.
20. H. Tao , W. Wei , X. Zeng , X. Liu, X. Zhang, Y. Zhang, *Michrochim Acta*, 166 (2009) 53.
21. G. Smith , R. Chen, S. Mapolie, *J. Organomet Chem.*, 673 (2003)
22. A.Salmon, P. Jutzi *J. Organomet. Chem.* 637–639 ( 2001) 595.
23. H. Xu Min, Z. Wei, Y. Pei Xie, X. Hai Ping, *Chinese chem. lett.*, 17 (2006) 1251.
24. J. Xu, *Journ.of Mat. Sci.*, 40 (2005) 2867.
25. D. Wang , Imae, Toyoko, Miki ,Masao, *Journal of colloid and Interface Science.*, 306 (2007) 222.
26. N.G.R. Mathebe, A. Morrin, E.I. Iwuoha, *Talanta*, 64 (2004) 115.
27. O.A. Arotiba, J.H. Owino, P.G. Baker, E.I. Iwuoha, *J Electroanal.l Chem.*, 638 (2010) 287.
28. A.Julio, Li Sun , Richard M, Crooks, *Chem Mater*, 14 (2002) 3995.
29. P. Yuehong, X. He , L. Xiaoyu, Hongliu Ding, C. Yuxiao , S. Guoyue , J. Litong, *Electrochem. Commun.*, 8 (2006) 1757.
30. A.-E. Radi, Sanchez,Josep Lluís Acero ;Baldrich Eva ; Sullivan,Ciara . *Anal.Chem.*, 77 (2005) 6320.
31. M.E. Orazem , B. Tribollet, *Electrochemical impedance spectroscopy*, Wiley (reprint 2008) Charppter 13.
32. M.S. B.Speiser In :A.J. Bard, P.R Unwin, *WILEY-VCH Verlag GmgH &Co. KGaA, Weinhein*, (2003) chapter 2.
33. O.A. Arotiba, O. Joseph, S. Everlyne, H. Nicolette , W. Tesfaye, J. Nazeem , P.G.L. Baker, ., E.I. Iwuoha, *Sensors*, 8 (2008) 6791.
34. Z. Wu, M. Guo, S.-B. Zhang, C.-R. Chen, J.-H. Jiang, G.-L. Shen, R.-Q. Yu, *Anal. Chem.*, 79 (2007) 2933.
35. Y.S. Kim, J.H. Niazi, M.B. Gu, *Anal Chim. Acta*, 634 (2009) 250.
36. Wu Z., Zheng Fan., G.-L. Shen , Ru-Qin Yu., *Biomaterials*, 30 (2009) 2950.
37. Y. Zhang, J.L. Zhou , B. Ning, *Water Research*, 41 (2007) 19.